

## Convective Activity over the Tibetan Plateau and Associated Atmospheric circulation during GAME-Tibet IOP

FUJIMAMI Hatsuki and YASUNARI Tetsuzo

Institute of Geoscience, University of Tsukuba. Ibaraki, 305-0821, Japan

### 1 Introduction

Convective activity over the Tibetan Plateau during the summer monsoon plays an important role in the atmospheric heating through the latent heat release (Nitta, 1983; Yanai et al., 1992 etc.). The convective activity shows remarkable diurnal variation and reaches maximum around 12Z (18 LST at 90°E) (Murakami, 1983; Yanai and Li, 1994). It is well known that convective activity during the summer monsoon is modulated by the intraseasonal variation over the Asian monsoon area (Yasunari, 1979; Murakami, 1984). The intraseasonal variation of convection is also found over the plateau (Fujinami and Yasunari, 2000). During GAME-Tibet IOP, the convection around mesoscale observation area shows the intraseasonal time scale variation with active and inactive period. This study focus on the intraseasonal time scale variation of convection over the Plateau and associated atmospheric circulation over and around the Tibetan Plateau.

### 2 Data

3-hourly IR-Tbb data derived from GMS-5 are used for the period of 27 May to 17 September 1998 to examine the convective activity. TBB data are obtained at  $1^\circ \times 1^\circ$  grid point. In order to determine the activity of convective clouds, we use the following index  $I_c$ , presented by Nitta and Sekine (1994), at each grid point defined by

$$\begin{aligned} I_c &= 250 - TBB && : TBB < 250 \text{ K} \\ I_c &= 0 && : Tbb \geq 250 \text{ K} \end{aligned}$$

where 250 K generally corresponds to the air temperature around 9000m above sea level over the plateau for the summer (JJA) and thus  $I_c$  represents an index for the deep convective clouds whose top height exceeds about 9000 m. The daily averaged NCEP/NCAR reanalysis data on  $2.5^\circ \times 2.5^\circ$  are also utilized to study the circulation fields and atmospheric stratification over and around the plateau.

### 3 Results

#### (1) Convective Activity

Figure 1 shows the horizontal distribution of  $I_c$  for the analysis period. The shading box denotes the Mesoscale observation area of GAME-Tibet. The region of high cloudiness shows the zonally-oriented distribution. Enhanced areas of convective activity are seen around 29°N, 87°E and 28°N, 100°E. Thus, the mesoscale observation area is located off the convection center. In order to reveal the seasonal and intraseasonal time scales variation of convective activity, the time series of the 5-day running mean  $I_c$  over the mesoscale observation area is

indicated in Fig. 2. Convective activity begins to enhance in mid-June and this enhancement is considered to be the onset of summer rainy season. After the onset, about 15-day fluctuation is prominent. This frequency is also confirmed in power spectrum of daily  $I_c$  time series by FFT method (not shown). The most active period can be seen in late August. After early September, convective activity weakens. Seasonal variation of radar echo-top height (30dBz) is similar to that of  $I_c$  (Yamada, 1999). This result indicates that the variation of  $I_c$  represents that of convective-type cloud with heavy rain. To examine the diurnal variation of the convection associated with the intraseasonal time scale variation, LST-seasonal cross section of 5-day running mean  $I_c$  is shown in Fig. 3. After mid-June, the diurnal variation of convective activity becomes prominent. Convective activity reaches the maximum around 18 to 21 LST throughout the analysis period. Minimum convection is found around 06 – 09 LST. It is interesting to note that the diurnal variation of convective activity is modulated on the intraseasonal time scales. Now, we choose the period from 24 to 28 August for

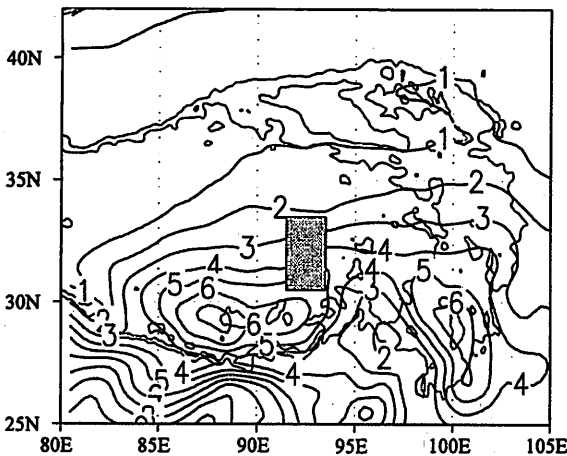


Fig. 1. Horizontal distribution of  $I_c$  averaged for the period from 27 May to 17 September 1998. Shading area denotes the Mesoscale observation area of GAME-Tibet.

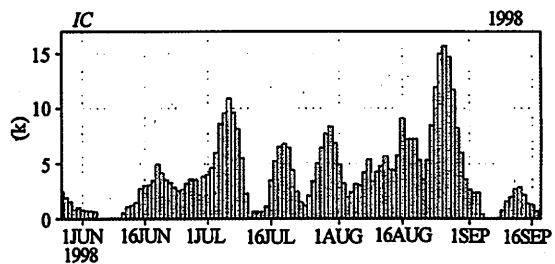


Fig. 2. The time series of the 5-day running mean  $I_c$  over the mesoscale observation.

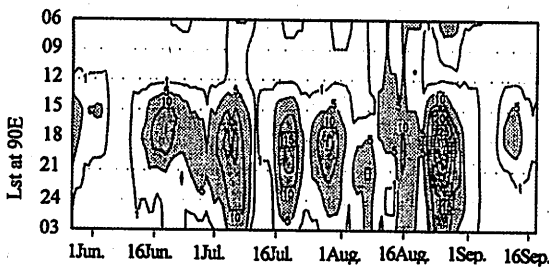


Fig. 3. LST-seasonal cross section of 5-day running mean  $I_c$  over the mesoscale observation area.

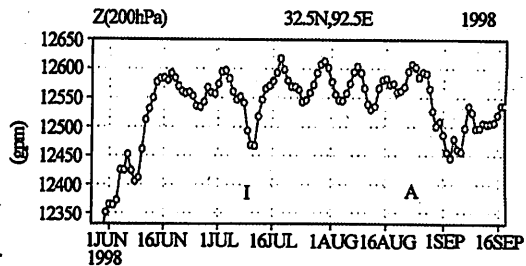


Fig. 4. Time series of geopotential height at 200 hPa for 32.5° N, 92.5° E. Selected periods for active and inactive convection are indicated "A" and "I", respectively.

active period and from 9 – 13 July as inactive period for the following case study in atmospheric circulation.

## (2) Atmospheric circulation

Figure 4 denotes the time series of geopotential height at 200 hPa near the grid of mesoscale observation area. In mid-June, geopotential height rises abruptly, which suggests the establishment of the Tibetan high over this area. This seasonal variation corresponds well with that of convective activity as shown in Fig. 2. In addition, it is evident that geopotential height fluctuates with the periodicity of about 15-day. Relative high (low) value of geopotential height is associated with active (inactive) period of convection between mid-June and late August.

In the active period, enhanced convection appears over the southern and central plateau in the evening (Fig. 5a). On the other hand, active convection is not observed to the west of 97°E all day long in the inactive period (Fig. 5b). This result suggests that the large-scale atmospheric circulation over and around the plateau controls cloud variation over the mesoscale observation area.

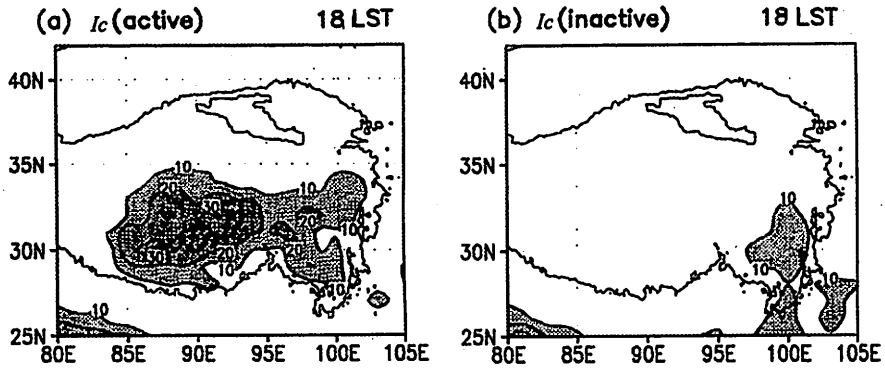


Fig. 5. Horizontal distribution of  $I_c$  for the (a) active and (b) inactive period at 18 LST.

Figure 6 indicates the geopotential height and wind vector at 200 hPa for the active and inactive period. During active period (Fig. 6a), the center of Tibetan high is located around 29°N, 90°E, While in the inactive period, the center is observed around 31°N, 60°E, and eastern edge of the high and the westerly trough covers over the plateau. Associated this geopotential height, northwesterly wind is dominant through 500 to 200 hPa over the Plateau.

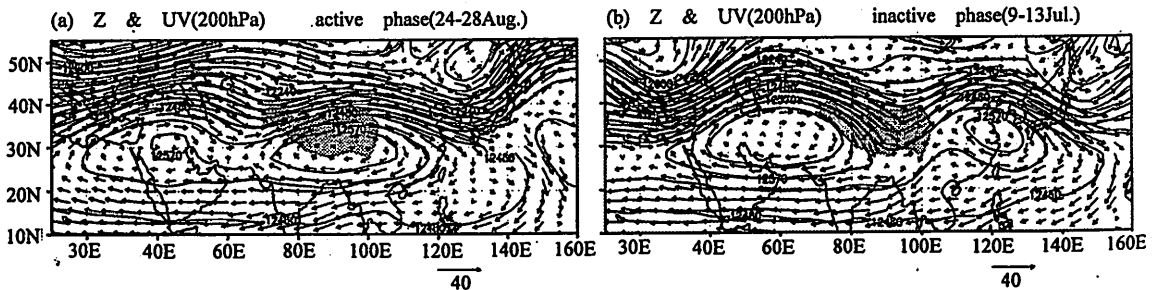


Fig. 6. Geopotential height and wind fields at 200 hPa for the (a) active and (b) inactive period.

To examine the characteristics of the lower atmospheric stratification, the stability for the moist convection of lower atmosphere and relative humidity at 500 hPa at 06 LST for the active

period are shown in Fig. 7a and b, respectively. Lower atmospheric stability is defined as the vertical difference of equivalent potential temperature between 400 and 500 hPa. Positive value indicates unstable condition for moist convection. In the active period, the lower stratification is unstable for moist convection from the morning. The value of relative humidity attains more than 90% across the large extent of the plateau. The lower atmosphere is very suitable condition for deep cumulus convection in the active period. On the other hand, in the inactive period, the lower atmosphere shows stable to the north of the central plateau and weak unstable over the southern part of the plateau. Dry air intrusion with less than 50% from the northwest of the plateau is observed. This result suggests that dry air intrusion due to northwesterly wind, as indicated in Figs. 6a – 6b, suppresses the active moist convection over the plateau.

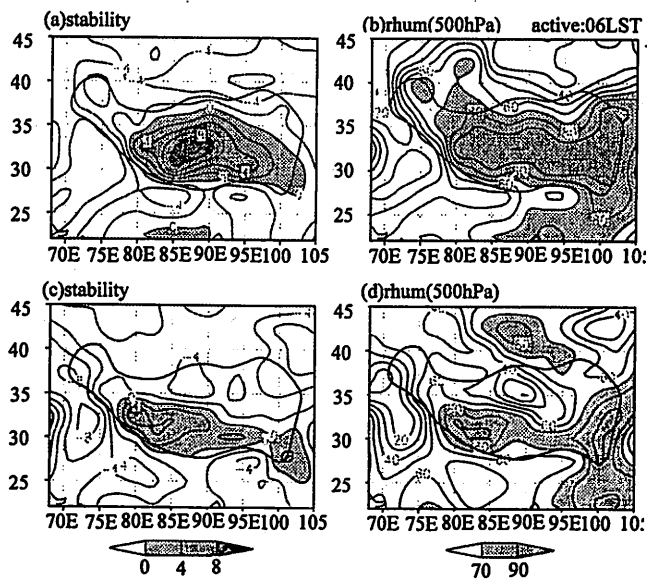


Fig. 7. (a) Vertical difference of equivalent potential temperature between 400 and 500hPa and (b) relative humidity at 500hPa at 06LST for the active period. (c) and (d) As in (a) and (b) but for inactive period.

## References

- Fujinami, H and T. Yasunari, 2000: Seasonal variation of the diurnal cloud activity over the Tibetan Plateau. (submitted to JMSJ and in revision).
- Murakami, M., 1984: Analysis of the deep convective activity over the western pacific and southeast Asia. Part II : Seasonal and intraseasonal variation during northern summer. *J. Meteor. Soc. Japan*, **62**, 88 – 108.
- Nitta, T., 1983: Observational study of heat sources over the eastern Tibetan Plateau during summer monsoon season. *J. Meteor. Soc. Japan*, **70**, 590 – 605.
- Yamada, H., 1999: Feature of radar echo over the Tibetan Plateau during GMAE-Tibet IOP, Proc. of the first international workshop on GAME-Tibet, 133 – 136.
- Yanai, M., C. Li and Z. Song, 1992: Seasonal heating of the Tibetan Plateau and its effects on the evolution of the Asian Monsoon. *J. Meteor. Soc. Japan*, **70**, 319 – 351.
- Yasunari, T., 1979: Cloudiness fluctuation associated with the northern hemisphere summer monsoon. *J. Meteor. Soc. Japan*, **57**, 227 – 242.